THE ASTROPHYSICAL JOURNAL, 469:954–963, 1996 October 1

THE HELICAL KINK INSTABILITY OF ISOLATED, TWISTED MAGNETIC FLUX TUBES

M. G. LINTON, D. W. LONGCOPE, AND G. H. FISHER
Space Sciences Laboratory, University of California, Berkeley, CA 94720
Received 1995 August 7; accepted 1996 April 16

ABSTRACT

To understand the dynamics of twisted active region flux tubes below the solar photosphere, we investigate the linear kink stability of isolated, twisted tubes of magnetic flux. We apply linearized equations of MHD to a cylindrical magnetic equilibrium (screw pinch), but with significant differences from earlier work. The magnetic field vanishes outside a radius $r = R$ where it is confined by the higher pressure of the unmagnetized plasma. The outside boundary of the tube is free to move, displacing the unmagnetized plasma as it does so. We concentrate on equilibria where all field lines have the same helical pitch: $B_\theta/rB_z = q = \text{const}$. The main results are as follows.

1. These equilibria are stable, provided that the field line pitch does not exceed a threshold; $q \leq q_{cr}$ for stability. The threshold is $q_{cr} = (\alpha)^{1/2}$, where α is the r^2 coefficient in the series expansion of the equilibrium axial magnetic field (B_z) about the tube axis ($r = 0$): $B_z(r) = B_0(1 - \alpha r^2 + \cdots)$. When this criterion is violated, there are unstable eigenmodes, $\xi \propto e^{i(\theta + kz)}$. The most unstable of these have a helical pitch k which is near (but not equal to) the field line pitch q.
2. For weakly twisted tubes ($qR \ll 1$) we derive growth rates and unstable eigenfunctions analytically. For strongly twisted tubes ($qR \gtrsim 1$), we find growth rates and unstable eigenfunctions numerically.
3. The maximum growth rate and range of unstable wavenumbers for a strongly twisted tube can be predicted qualitatively by using the analytical results from the weakly twisted case. The maximum growth rate in that case is given by $\omega_{max} = v_A R(q^2 - q_{cr}^2)/3.83$, where v_A is the axial Alfvén speed. The range of unstable wavenumbers is $(-q - \Delta k/2) < k < (-q + \Delta k/2)$, where $\Delta k = 4qR(q^2 - q_{cr}^2)^{1/2}/3.83$.
4. The kink instability we find consists mainly of internal motions. Helical translations of the entire tube are stable.
5. We argue that an emerging, twisted magnetic flux loop will tend to have a uniform q along its length. The increase in the tube radius R as it rises results in a decreasing value of q_{cr}. This means that the apex of the flux loop will become kink unstable before the rest of the tube.
6. Our results suggest that most twisted flux tubes rising through the convection zone will be stable to kinking. Those few tubes which are kink unstable, and which presumably become knotted or kinked active regions upon emergence, only become kink unstable some time after they have begun rising through the convection zone.

Subject headings: instabilities — MHD — Sun: activity — Sun: interior — Sun: magnetic fields

1. INTRODUCTION

The greatest concentrations of magnetic flux on the Sun, known as "active regions" or "bipolar magnetic regions," consist of two adjacent areas of opposite magnetic polarity; the magnetic field lines connecting the two polarities rise into the corona, resulting in the "coronal loops" seen in X-ray images of the Sun. This morphology suggests that the magnetic flux visible at the surface results from the emergence of loops of flux from the solar interior. In current theories of the solar cycle dynamo (see, e.g., review by DeLuca & Gilman 1991; Hughes 1992), magnetic flux is generated in a shear layer near the base of the solar convection zone. From here, it emerges in the form of discrete "magnetic flux tubes," the topmost portions of which form bipolar magnetic regions where the fields pierce the photosphere, while the remainder of the tube stays anchored at the base of the convection zone.

Recent theoretical work on the dynamics of emerging flux tubes, based on the "thin flux tube" approach outlined by Spruit (1981), has been successful in reproducing many of the observed properties of solar active regions. The thin flux tube approximation assumes that a magnetic flux tube diameter is small compared to all other relevant size scales *and* that the distribution of physical properties across the tube can be replaced by simple averages. Applying these approximations to the equations of ideal magnetohydrodynamics (MHD) yields a nonlinear model for the dynamical evolution of a thin flux tube. In recent numerical solutions of these model equations, loops emerge to form bipoles which are tilted relative to the equator, in agreement with observation. The tilt angles in the simulations vary with latitude (the so-called "Joy's Law" [Zirin 1988, p. 307;—see also D'Silva & Choudhuri 1993]), and with the total unsigned flux (Fan, Fisher, & McClymont 1994) in quantitative agreement with observation (Fisher, Fan, & Howard 1995). In addition, observed morphological differences between leading and following sides of the bipole are also present in the numerical simulations (Fan, Fisher, & DeLuca 1993; Moreno-Insertis, Caligari, & Schüssler 1994; Caligari, Moreno-Insertis, & Schüssler 1995).

Most models have considered only untwisted flux tubes. In an untwisted tube, all field lines parallel the tube's axis exactly, and there is no current or twist in that direction. However, an untwisted tube lacks integrity and will be fragmented or dispersed by external hydrodynamic forces (Parker 1979a; Schüssler 1979). Recent simulations of self-consistent buoyant evolution indicate that an initially untwisted tube will split into two counterrotating elements before it rises several of its own diameters (Longcope, Fisher, & Arendt 1995). To remain intact, the flux tube must

be twisted sufficiently that the shear Alfvén speed around its own axis is as great as its speed of buoyant rise through the atmosphere.

While it provides integrity to the tube, axial current can also lead to dynamical behavior quite different from that of the untwisted flux tube. It is well known that a cylindrical equilibrium containing both axial and azimuthal fields is subject to a class of current driven instabilities known as *kink modes* (see, e.g., Shafranov 1957; Kruskal et al. 1958). This instability results in a displacement of the magnetic axis into a helix with a pitch similar to the twist of the field lines themselves. Once the axis and the circular boundary of the flux tube has developed a helical pitch, the flux tube itself is said to be *kinked*. Care must be taken to distinguish the helical *twist* of the individual field lines from the helical *kink* of the tube itself, which results from the kink instability. (In MHD, the term *kink* has generally referred to such current-driven instabilities. The term has also been used to describe a buoyancy-driven instability of an initially horizontal, but untwisted tube [Moreno-Insertis 1986]. Here, we use the term exclusively in the first of these senses.) Although the nonlinear development of the kink instability has yet to be treated rigorously in an isolated flux tube, it is likely to distort the axis of the tube severely. The emergence of such a tube will result in a bipolar region with properties quite different from those of a simple untwisted flux tube.

Most active regions do not exhibit strong signs of magnetic twist and appear consistent with the emergence of simple loops of flux. However, there is a small but important subset of loops that are significantly twisted and possibly kinked or knotted when they emerge. The structure and dynamics of these active regions is especially important because they are linked to the occurrence of large solar flares. The link between flares and emerging, kinked flux loops can be inferred from the fact that the "island δ" spot configuration is typically the site of the largest solar flares (see, e.g., Zirin 1988, p. 337). Here, two spot umbrae of opposite polarity emerge within one spot penumbra; further, the orientation of the two polarities is frequently reversed from the usual Hale configuration. One interpretation of δ spots is that a rising loop of a twisted flux tube has kinked into a braided structure, similar to that which results when twist is applied to the loop of a rubber band. This would account qualitatively for the reversed polarity configuration, the close proximity of the opposite polarity spots, and the occurrence of flares as the oppositely directed fields in the intertwined loop legs undergo reconnection.

Detailed observations of flare productive active regions support this view. Kurokawa et al. (1994) studied the development of flaring active region NOAA 7270 from 1992 September 5 to 7 with high-resolution Hα images, magnetograms, and soft X-ray images from *Yohkoh*. They found that magnetic shear observed with the vector magnetograms was caused by the successive emergence of twisted flux ropes from below the photosphere. Similarly, in the analysis of the legendary 1972 August flaring active region, Tanaka (1991) found that the time evolution of this δ spot group could be explained by the emergence of a twisted flux loop which had actually formed a knot like structure. Kurokawa (1991) reviews a number of other observations in which flare productive active regions develop through the emergence of twisted flux tubes. Most recently, Leka (1995, p. 76) observed the emergence of new magnetic flux in the flare-productive active region NOAA 7260 with the Imaging Vector Magnetograph at the University of Hawaii's Mees Solar Observatory and found that emerging bipoles were in the shape of helically twisted loops of flux.

This suggests that a δ spot group represents the emergence of a flux tube that not only has twisted fields, but has also succumbed to an MHD kink instability that distorted its axis. To explore this possibility and its consequences, it is essential to develop a nonlinear model for the evolution of a thin, twisted flux tube. For cases of relatively weak twist (azimuthal magnetic field), initial estimates suggest that the tube's dynamics will be altered only slightly from those of an untwisted tube. The twist can then be treated as a linear perturbation, giving rise to eigenmodes including torsional Alfvén waves (Ferriz-Mas & Schüssler 1990). These have little or no effect on the gross dynamics, and thus the tube as a whole would behave essentially as if it were untwisted. However, if the linear modes resulting from the twist are dynamically unstable (i.e., to a kink mode), they would almost certainly affect the large-scale dynamics.

This paper establishes the conditions under which an isolated, twisted flux tube is linearly unstable to kinking. We use the term "thin" for our twisted tube in one of the senses that it is applied to untwisted flux tubes; namely, that the radius of its cross section R is negligible compared to length scales in the external medium, compared to scales of variation along the tube, and compared to the curvature of its axis. In a twisted tube, a magnetic field line twists about the central axis of the tube with some pitch q. We refer to a case where $qR \ll 1$ as a *weakly twisted* tube. In this case, the axial length for one turn, $2\pi/q$, will also be much larger than the tube's radius. We will not, however, restrict ourselves to the limit of weak twist, since the general criterion for kink instability will turn out to be $qR = O(1)$.

Treatments of untwisted thin tubes often use only the cross-sectional averages of quantities like axial magnetic field and internal pressure, which is similar to keeping only leading order terms from a Taylor expansion in radius r. However, the dynamics of a kink mode depend on the detailed distribution of magnetic field and pressure with radius. Therefore, it will be necessary for us to work with a variety of flux tube *profiles*.

To separate the kink instability from the general dynamics of the flux tube, we consider a tube which is initially in equilibrium. We take a straight tube with perfect symmetry along its axis, $\hat{z}$ (i.e., a cylinder) immersed in a uniform external medium which is unmagnetized but perfectly conducting. This equilibrium represents the lowest order in an "inverse aspect ratio" expansion of a more general flux tube. Subsequent terms in such an expansion will be smaller by factors R/L, where L is some axial length scale.

The stability of such an equilibrium has been studied extensively in the contexts of the laboratory (e.g., Shafranov 1957; Kruskal et al. 1958; Suydam 1959; Voslamber & Callebout 1962) and the solar corona (e.g., Gold & Hoyle 1960; Anzer 1968; Raadu 1972; Hood & Priest 1980, 1981; Migliuolo & Cargill 1983; Craig et al. 1990); our treatment generally parallels that analysis. In § 2 we review the variational principle for linear stability to ideal MHD perturbations (Bernstein et al. 1958). We use a generalization of this method to find the linear growth rates and eigenmodes as well as the criteria for marginal stability. Helical perturbations of arbitrary radial structure, $\xi(r)$, result in a second-order differential equation of the Sturm-Liouville type for the eigenmodes. Our case differs from the laboratory and coronal analyses in its treatment of the tube's outer bound-

ary. This boundary, which separates the magnetized plasma inside the tube from the unmagnetized plasma outside, is a free surface which must be permitted to move in response to the perturbation. As there is no field outside this free surface, in contrast to many other studies of the kink mode, the tube carries no net current. In § 2.3 we derive the boundary condition for the eigenmode equation which describes this free surface, and compare it to boundary conditions appropriate in other contexts.

In § 3 the eigenmode equation is solved analytically in the limit of a weakly twisted tube. The solution shows that tubes are unstable to kinking provided their pitch q exceeds a threshold q_{cr} that depends on the field profile of the equilibrium. The helical pitch k of the unstable eigenmode closely matches, but does not equal q. The eigenmode's cross-sectional variation is mainly internal, distorting the axis of the tube much more than the boundary. Thus, the free boundary assumption does not significantly affect the dynamics of *weakly* twisted tubes, as the weakly twisted eigenmodes require very little boundary motion.

The threshold for marginal stability q_{cr} depends on the equilibrium field profile. For the most plausible profiles, $q_{cr} \sim 1/R$. Thus for a tube to be unstable, i.e., $q \geq q_{cr}$, it cannot be weakly twisted. This also means that the onset of instability for an infinitely long, current neutral tube with a free boundary depends on *both* its twist and tube radius, in contrast to cases where the instability depends on only the twist, or on the total number of turns (e.g., Shafranov 1957: Hood & Priest 1980, 1981). In § 4, we treat numerically a class of strongly twisted flux tubes. These are found to behave qualitatively like their weakly twisted counterparts, but with correspondingly larger growth rates and larger distortions of the tube boundary. Thus the free boundary assumption, though unimportant in the weakly twisted limit, becomes increasingly important for strongly twisted tubes. Strongly twisted tubes are more likely to kink, and will kink more strongly than weakly twisted tubes. In § 5 we show that a flux tube which starts out weakly twisted and kink stable deep in the convection zone can become kink unstable as it rises. This results from the tube's expansion, and the subsequent decrease in q_{cr}. Estimates of the linear growth rates for a typical tube indicate that the kink mode can e-fold several times during its rise.

2. THE LINEAR EIGENMODE ANALYSIS

2.1. *Energy Principle*

The energy principle is a method for evaluating the linear stability of a MHD equilibrium subjected to a small displacement perturbation $\boldsymbol{\xi}$. We choose a cylindrically symmetric magnetic equilibrium (i.e., independent of both θ and z in cylindrical coordinates). It consists of a tube plasma with magnetic field $\boldsymbol{B}_0(r)$:

$$\boldsymbol{B}_0(r) = [0, B_\theta(r), B_z(r)] , \tag{1}$$

surrounded by field-free plasma, and confined by the higher pressure of this external plasma. The field vanishes outside the boundary of the tube, $r = R$. In many cases, the field will be formally discontinuous at the boundary, but this is meant to represent a smooth transition to zero over a distance small compared to R.

If an energy integral, $W[\boldsymbol{\xi}, \boldsymbol{B}_0(r)]$, representing the second-order variation of potential energy, is less than zero, then the equilibrium $\boldsymbol{B}_0(r)$ is unstable to the perturbation $\boldsymbol{\xi}$. The energy integral as derived by Bernstein et al. (1958) is

$$W = -\tfrac{1}{2}\int d^3x \boldsymbol{\xi}^* \cdot \boldsymbol{F}(\boldsymbol{\xi}), \tag{2}$$

where $\boldsymbol{F}$ is the force per unit volume from the linearized MHD equations. The perturbation $\boldsymbol{\xi}$ is related to the velocity by $\boldsymbol{v} = d\boldsymbol{\xi}/dt$.

Evaluating $\boldsymbol{F}$ and substituting into W, we find all boundary terms are zero because $\boldsymbol{B}_0(r) = 0$ outside the tube (see Bateman 1978, p. 96). The most unstable modes are incompressible (Newcomb 1960), so hereafter we assume incompressibility, and drop terms proportional to $\nabla \cdot \boldsymbol{\xi}$ in the energy integral to give ((Newcomb 1960):

$$W = \frac{1}{2}\int d^3x \left[\frac{|\boldsymbol{Q}|^2}{4\pi} - \frac{1}{c}\boldsymbol{\xi}^* \cdot (\boldsymbol{J}_0 \times \boldsymbol{Q})\right], \tag{3}$$

where $\boldsymbol{Q} = \nabla \times [\boldsymbol{\xi} \times \boldsymbol{B}_0(r)]$, $\boldsymbol{J}_0 = c\nabla \times \boldsymbol{B}_0(r)/4\pi$, and $\boldsymbol{B}_0(r)$ is the unperturbed magnetic field. Lagrangian coordinates are used to permit a discontinuity in $\boldsymbol{B}_0(r)$ at the boundary; the perturbed field strength $\boldsymbol{B}_1(r)$ is formally divergent there in an Eulerian formulation. This involves expressing ∇ in Lagrangian coordinates, and $\boldsymbol{B}_1 \rightarrow \boldsymbol{Q} + (\boldsymbol{\xi} \cdot \nabla)\boldsymbol{B}_0(r)$ (Bernstein et al. 1958). In contrast, the Eulerian perturbation is $\boldsymbol{B}_1 = \boldsymbol{Q}$ (Bateman 1978, p. 92). Note that the plasma pressure, which balances magnetic forces in the tube, does not appear in this expression.

While instability follows from the sign of W for a particular $\boldsymbol{\xi}$, the unstable growth rate must be found from constrained variation over all neighboring perturbations. In particular, an eigenmode will extremize W while holding fixed the integral (Bateman 1978, p. 98)

$$K = \frac{1}{8\pi}\int d^3x |\boldsymbol{\xi}|^2 . \tag{4}$$

This constrained variation is accomplished by finding an extremum of a generalized energy $U = W + \lambda K$, where λ is a Lagrange multiplier. At an extremum λ is related to the eigenfrequency,

$$\lambda = -4\pi\rho_0\omega^2 , \tag{5}$$

where $\boldsymbol{\xi} \propto e^{iwt}$. A negative ω^2 (positive λ) implies an instability with growth rate $|\omega|$.

2.2. *Variation of U*

We focus on the kink mode (azimuthal mode number $m = 1$), and take $\boldsymbol{\xi}$ to have helical symmetry, with pitch k, and an arbitrary radial structure for which we will solve by variation:

$$\boldsymbol{\xi} = [\xi_r(r), \xi_\theta(r), \xi_z(r)]e^{i(kz+\theta)}. \tag{6}$$

All three components of the perturbation must be varied, but they are interrelated by incompressibility

$$\nabla \cdot \boldsymbol{\xi} = 0 = \frac{d\xi_r}{dr} + \frac{\xi_r}{r} + i\frac{\xi_\theta}{r} + ik\xi_z . \tag{7}$$

Using this to eliminate $\xi_z(r)$ gives an expression for the generalized energy

$$U = \frac{L}{4}\int r\,dr \left[\xi_r^2\left\{\lambda + [\boldsymbol{k} \cdot \boldsymbol{B}_0(r)]^2 + \frac{2B_\theta^2}{r^2} - \frac{1}{r}\frac{dB_\theta^2}{dr}\right\}\right.$$
$$+ 4\frac{i\xi_\theta}{r}\xi_r B_\theta \boldsymbol{k} \cdot \boldsymbol{B}_0(r) + \{\lambda + [\boldsymbol{k} \cdot \boldsymbol{B}_0(r)]^2\}$$
$$\left.\times\left[(i\xi_\theta)^2 + \frac{(\xi_r' + \xi_r/r)^2}{k^2} + \frac{2i\xi_\theta}{r}\frac{(\xi_r' + \xi_r/r)}{k^2} + \frac{(i\xi_\theta/r)^2}{k^2}\right]\right], \tag{8}$$

where L is the length of the tube, $\dot{\xi}_r \equiv d\xi_r/dr$, and $[\boldsymbol{k}\cdot\boldsymbol{B}_0(r)] = kB_z + B_\theta/r$.

The integrand in equation (8), call it $\mathscr{A}(\xi_r, \dot{\xi}_r, \xi_\theta)$, does not depend on $\dot{\xi}_\theta$. A variation over ξ_θ yields the simple Euler-Lagrange equation $\partial\mathscr{A}/\partial\xi_\theta = 0$, which can then be used along with equation (7) to express ξ_θ and ξ_z in terms of the radial displacement alone:

$$\xi_\theta = \frac{ir}{1+k^2r^2}\left\{\dot{\xi}_r + \frac{\xi_r}{r} + \frac{2k^2\xi_r B_\theta \boldsymbol{k}\cdot\boldsymbol{B}_0(r)}{\lambda + [\boldsymbol{k}\cdot\boldsymbol{B}_0(r)]^2}\right\} \tag{9}$$

$$\xi_z = \frac{ikr^2}{1+k^2r^2}\left[\dot{\xi}_r + \frac{\xi_r}{r} - \frac{2\xi_r B_\theta \boldsymbol{k}\cdot\boldsymbol{B}_0(r)}{r^2\{\lambda + [\boldsymbol{k}\cdot\boldsymbol{B}_0(r)]^2\}}\right] \tag{10}$$

Using expression (9) for ξ_θ in equation (8) gives a generalized energy

$$U = \frac{L}{4}\int dr(f\dot{\xi}_r^2 + g\xi_r^2)\,, \tag{11}$$

where the coefficients depend on the specific form of the equilibrium as well as on the eigenvalue λ:

$$f = \frac{r^3\{\lambda + [\boldsymbol{k}\cdot\boldsymbol{B}_0(r)]^2\}}{1+k^2r^2}\,, \tag{12}$$

$$g = \frac{k^2r}{1+k^2r^2}\left[r^2\{\lambda + [\boldsymbol{k}\cdot\boldsymbol{B}_0(r)]^2\} - r\frac{d|\boldsymbol{B}_0(r)|^2}{dr} - 2B_\theta^2\left\{\frac{2[\boldsymbol{k}\cdot\boldsymbol{B}_0(r)]^2}{\lambda + [\boldsymbol{k}\cdot\boldsymbol{B}_0(r)]^2} - 1\right\} + \frac{2}{1+k^2r^2}(r^2\lambda + k^2r^2B_z^2 - B_\theta^2)\right]. \tag{13}$$

Minimizing U with respect to $\xi_r(r)$ results in the Euler-Lagrange equation,

$$\frac{d}{dr}f\frac{d\xi_r}{dr} - g\xi_r = 0\,. \tag{14}$$

This can be solved, subject to appropriate boundary conditions (discussed below) to give ξ_r, and therefore ξ_θ and ξ_z. The boundary conditions at $r = 0$ and $r \to \infty$ can be satisfied only for specific values of λ, which enters equation (14) implicitly through f and g. This determines the growth rates which characterize the stability of the tube, to be discussed in §§ 3–4. For most cases, the eigenmode consists primarily of a cross-sectional swirling motion (ξ_r and ξ_θ) with a small axial motion (ξ_z).

Equation (14) is singular if $f(r)$ vanishes, which can occur for stable ($\lambda < 0$) and for marginally stable cases ($\lambda = 0$). The latter singularity occurs at the radius where $\boldsymbol{k}\cdot\boldsymbol{B}_0(r) = 0$, called the *mode resonant surface*. In such a case, ξ_r can be discontinuous, permitting internal (external) instabilities in which $\xi_r \equiv 0$ outside (inside) the mode rational surface (see Rosenbluth, Dagazian, & Rutherford 1973 for a discussion of the internal kink mode). For the case of instability ($\lambda > 0$), equation (14) is formally nonsingular, but often the mode resonant surface remains the site of a steep gradient in ξ_r. In this way, the inertia "resolves" the singularity at the resonance in an internal kink mode (Rosenbluth et al. 1973).

Equations (11)–(13) apply to any cylindrical MHD equilibrium and have been studied in many contexts (Newcomb 1960; Rosenbluth et al. 1973, both with $\lambda = 0$). Application to a flux tube neglects curvature of its axis and variations in atmospheric properties. Thus, we implicitly assume a flux tube that is "thin" in the commonly used sense (Spruit 1981): a radius much smaller than both the axial radius of curvature and the pressure scale height of the atmosphere.

The functions $f(r)$ and $g(r)$ depend on the specifics of the tube equilibrium $\boldsymbol{B}_0(r)$ defined in equation (1). Any pair of field profiles $B_\theta(r)$ and $B_z(r)$ constitutes a valid equilibrium when supplemented with the appropriate pressure profile, $p(r)$. Since only incompressible perturbations were considered, the function $p(r)$ never enters the analysis explicitly, meaning that both magnetic field profiles are arbitrary. In contexts where $\beta \equiv 8\pi p/|B|^2$ is much less than unity, such as the corona, the pressure is unable to balance magnetic forces, and force-free equilibria, including the well-known Gold-Hoyle field (Gold & Hoyle 1960), are typically considered.

Deep in the convection zone, a flux tube has a large $\beta(\sim 10^6)$ so magnetic forces are of little importance in determining equilibrium structure. Thus, pressure, temperature, and density profiles must all be almost perfectly flat. If a tube begins in an untwisted state with some axial magnetic field profile $B_z(r)$, then simple twisting will not change this profile. This follows from the ideal MHD constraint $B_z/\rho =$ *constant* which holds provided flow along the axis is small during the twisting. Therefore, twisting a flux tube to have pitch q changes only the azimuthal field, $B_\theta(r)$.

$$B_\theta(r) = qrB_z(r)\,, \quad r \le R\,, \tag{15}$$

where $B_z(r)$ is the axial field profile before and after twisting. Equilibria of this form are most relevant for our present discussion; however, to aid comparisons with previous work on force-free equilibria, we continue to consider more general profiles until § 3.

2.3. *Boundary Conditions on $\xi_r(r)$*

Regularity at the origin, requires $\dot{\xi}_r(0) = 0$ and $\xi_r(0)$ be a constant, which can be taken as unity without loss of generality. The outer boundary of the tube $r = R$ is not actually a boundary of the problem. It is simply a point beyond which the magnetic field is known to vanish; it might be the location of a discontinuity in the equilibrium magnetic field. The Euler-Lagrange equation (14) represents the linearized MHD equations and is valid at points where $\boldsymbol{B}_0(r)$ is both finite and zero (i.e., both inside and outside the tube). The true outer boundary condition is that ξ_r vanish as $r \to \infty$.

Even if the equilibrium is discontinuous at $r = R$, the Euler-Lagrange equation (14) must hold across the boundary, and

$$\int_{R_-}^{R_+} dr\left[\frac{d}{dr}\left(f\frac{d\xi_r}{dr}\right) - g\xi_r\right] = 0\,. \tag{16}$$

Equation (16) can be nontrivial as a result of the delta function in $d\boldsymbol{B}_0(r)/dr$ at $r = R$. This results in the following equation which must be satisfied at the outer radius of the tube:

$$k^2|\boldsymbol{B}_0(R)|^2\xi_r(R) + R\{\lambda + [k\cdot\boldsymbol{B}_0(R)]^2\}\dot{\xi}_{r_{in}}(R) - R\lambda\dot{\xi}_{r_{out}}(R) = 0\,, \tag{17}$$

where $\dot{\xi}_{r_{in}}(R)$ and $\dot{\xi}_{r_{out}}(R)$ are $\dot{\xi}_r(R)$ from the internal and external solutions of equation (14), respectively.

This boundary condition accounts for an interaction between the magnetized tube and the unmagnetized external medium. The response of the unmagnetized medium is contained in the external solution treated below. Previous

stability analyses relevant to tokomaks or coronal loops have used different forms of external boundary conditions. For those cases, the tube is confined by a conducting wall, $\xi_r(R) = 0$ (see, e.g., Voslamber & Callebout 1962), or an external vacuum field $\boldsymbol{B}(r > R) \neq 0$ (Kruskal et al. 1958; Anzer 1968; Hood & Priest 1981). Neither of these is relevant to our study of the convection zone, where tubes have free boundaries and essentially no external magnetic field.

The boundary condition given by equation (17) is equivalent to requiring that the total pressure, $P = p + B^2/8\pi$, be continuous across the boundary. While it was not necessary to solve explicitly for the pressure, we can do so after the fact. Taking the $\hat{z}$ component of the linearized MHD momentum equation in Lagrangian coordinates, and expressing P as the equilibrium P_0 plus the perturbed pressure P_1 gives

$$P_1 = \frac{i}{4\pi k}\{\lambda + [\boldsymbol{k}\cdot\boldsymbol{B}_0(r)]^2\}\xi_z - \frac{B_\theta^2}{4\pi r}\xi_r . \tag{18}$$

Using equation (10) to express ξ_z in terms of ξ_r and $\dot{\xi}_r$ and requiring P to be continuous at R returns equation (17). In Lagrangian coordinates, continuity of P is equivalent to continuity of P_1, whereas in Eulerian coordinates a motion of the boundary introduces a discontinuity in P_0 arising from an initial discontinuity in $\dot{P}_0$. This discontinuity must be offset by a discontinuity in P_1. In his study of flux tube stability, Roberts (1956) applied the condition of pressure continuity, but this was done in Eulerian coordinates.

Outside the tube where $\boldsymbol{B}_0(r) = 0$, equation (14) can be solved analytically for $\xi_r(r)$. The solutions are consistent with requiring ξ_r to be the gradient of a harmonic scalar potential (i.e., $\boldsymbol{\xi}$ is divergence-free and curl-free outside the tube. The scalar potential is then related to the pressure P_1.) The external solution of equation (14) for ξ_r is

$$\begin{aligned}\xi_{r_{\rm out}}(r) &= -a|k|\dot{K}_1(|kr|)\\ \dot{\xi}_{r_{\rm out}}(r) &= -k^2 a\ddot{K}_1(|kr|),\end{aligned} \tag{19}$$

where K_1 is a modified Bessel function, and a is a constant. The other independent solution, the modified Bessel function I_1, is rejected because it diverges at large distances and is therefore inconsistent with a localized perturbation. Since $\xi_r(r)$ must be continuous across the boundary, $\xi_{r_{\rm in}}(R) = \xi_{r_{\rm out}}(R) = \xi_r(R)$, and we can express $\dot{\xi}_{r_{\rm out}}(R)$ as

$$\dot{\xi}_{r_{\rm out}}(R) = \frac{|k|\ddot{K}_1(|kR|)}{\dot{K}_1(|kR|)}\xi_{r_{\rm in}}(R) = -\frac{1}{R} \times\left[1 + \frac{(1+k^2R^2)K_1(|k|R)}{|k|RK_0(|k|R) + K_1(|k|R)}\right]\xi_{r_{\rm in}}(R) . \tag{20}$$

Equation (17) then gives a linear, homogeneous boundary condition for the internal solution

$$D(\lambda; R, k) = \left[k^2|\boldsymbol{B}_0(r)|^2 + \lambda + \lambda \times\frac{(1+k^2R^2)K_1(|k|R)}{|k|RK_0(|k|R) + K_1(|k|R)}\right]\xi_r(R) + \{R\lambda + R[\boldsymbol{k}\cdot\boldsymbol{B}_0(r)]^2\}\dot{\xi}_{r_{\rm in}}(R) = 0 . \tag{21}$$

The function $D(\lambda; R, k)$ can be regarded as a "dispersion function" for the eigenvalue λ. It depends parametrically on R and k and implicitly on the equilibrium $\boldsymbol{B}_0(r)$. Equation (21) forces the solution to match continuously to a potential solution decaying at infinity and remains valid even if the magnetic field goes continuously to zero at $r = R$.

3. ANALYTICAL RESULTS

3.1. *The Weakly Twisted Limit*

To apply the boundary condition (eq. [21]), ξ_r must be found by integrating the Euler-Lagrange equation (eq. [14]) out from the axis. This equation simplifies significantly when $qR \ll 1$, the *weakly twisted* flux tube. It can be shown a posteriori that such tubes are unstable only to perturbations with similarly weak helical pitch $|k|R \ll 1$. Further, these tubes are unstable only if $B_z(r)$ and $B_\theta(r)$ vary slowly with radius; thus, it is possible to use only the lowest orders in Taylor series expansions

$$\begin{aligned}B_z &= B_0(1 - \alpha r^2)\\ B_\theta &= B_0 qr ,\end{aligned} \tag{22}$$

where $B_0 = |\boldsymbol{B}_0(0)|$, and $\alpha R^2 \ll 1$. Again, the field (eq. [22]) is not necessarily force-free, although for $\alpha = q^2$ it is force-free to lowest order. In non–force-free cases, zero order magnetic forces are balanced by plasma pressure gradients in the tube.

In the weakly twisted limit, the dispersion relation (eq. [21]) reduces to

$$D(\lambda; R, k) = (k^2B_0^2 + 2\lambda)\xi_r(R) + [\lambda + B_0^2(k+q)^2]R\dot{\xi}_{r_{\rm in}}(R) = 0 . \tag{23}$$

This has an immediate interpretation for $\xi_r(r)$ which are nearly uniform across the tube, i.e., $\xi_r(R)/R \gg \dot{\xi}_r(R)$. In this case, equations (23) and (5) give us

$$\lambda = -\frac{k^2}{2}B_0^2 \quad\text{or}\quad \omega = \pm\frac{k}{\sqrt{2}}\sqrt{\frac{B_0^2}{4\pi\rho_0}} = \pm\frac{kv_A}{\sqrt{2}}, \tag{24}$$

where v_A is the Alfvén speed at $r = 0$. The phase speed of this mode is the tube wave speed $v_A/2^{1/2}$ (Priest 1984, p. 112), differing from the Alfvén speed by a factor of $1/2^{1/2}$ due to the "added mass" effect (Ryutov & Ryutova 1976; Spruit 1981). The tube is therefore stable to perturbations of relatively uniform $\xi_r(r)$, which propagate as Alfvén waves. *This tells us that if any perturbations are unstable, they will require large variations in ξ_r across the tube, and hence will correspond primarily to internal motion.*

The modes to which the tube is unstable have a helical pitch closely matched to that of the magnetic field, $k \simeq -q$, and have growth rates much smaller than the Alfvén frequency, $\lambda \ll k^2B_0^2$. In this limit equation (14) becomes

$$\frac{d}{dr}\left(r^3\frac{d}{dr}\xi_r\right) + g_0 r^3\xi_r = 0 , \tag{25}$$

where $g_0 = -g/f$ has a simple form in the weakly twisted limit

$$g_0 = \frac{4q^2}{\tilde{\lambda}+\eta^2}\left(\frac{q^2\eta^2}{\tilde{\lambda}+\eta^2} - \alpha\right). \tag{26}$$

Here the mismatch between q and $-k$ is written as η:

$$\eta \equiv q + k \ll q , \tag{27}$$

and $\tilde{\lambda}$ is the squared frequency normalized to the Alfvén velocity squared,

$$\tilde{\lambda} \equiv \frac{\lambda}{B_0^2} = -\frac{\omega^2}{v_A^2} \ll q^2 . \tag{28}$$

The solution of the weakly twisted Euler-Lagrange equation (eq. [25]) is

$$\xi_r(r) = \frac{2}{\sqrt{g_0}\, r} J_1(\sqrt{g_0}\, r) , \tag{29}$$

where J_1 is the Bessel function of the first kind. For $g_0 < 0$, the argument of J_1 is imaginary, and $\xi_r(r)$ will be proportional to I_1. In this case $\xi_r(r)$ and its derivative will always have the same sign, and $D(\tilde{\lambda}) = 0$ cannot be satisfied for positive $\tilde{\lambda}$. Therefore, instability occurs only when $g_0 > 0$. In light of the definition (eq. [26]) this indicates that *there is a minimum twist a tube must have to be kink unstable:*

$$q > q_{cr} \equiv \sqrt{\alpha} \text{ for instability} . \tag{30}$$

Equation (30) has several important consequences. First, a thin, weakly twisted tube will be unstable only if the $B_z(r)$ profile is almost flat. The ratio of axial field strength at the edge to that on the axis is

$$\frac{B_z(R)}{B_z(0)} = 1 - \alpha R^2 , \tag{31}$$

which is close to unity given that $\alpha R^2 \ll 1$. Indeed, this verifies a posteriori that a series expansion of the field profile is sufficient for a weakly twisted tube. However, it is unlikely that a real flux tube could maintain such a perfectly flat profile in the face of thermal and resistive diffusion. Nor would it be likely to even begin so flat before diffusion had occurred. For this reason, we conclude that it is unlikely that weakly twisted flux tubes will kink. Nevertheless, this limit will form a valuable touchstone for the strongly twisted tubes discussed in §§ 3.2 and 4, so we continue the analysis.

Applying the boundary condition (eq. [21]) to the weakly twisted solution for $\xi_r(r)$ (eq. [29]) and taking limits $\eta \ll q$ and $\tilde{\lambda} \ll q^2$ result in the condition

$$J_2(\sqrt{g_0}\, R) = \frac{k^2}{\sqrt{g_0}\, R(\tilde{\lambda} + \eta^2)} J_1(\sqrt{g_0}\, R) . \tag{32}$$

This a transcendental equation for the eigenfrequency, $\tilde{\lambda}$, in terms of k (or equivalently $\eta = k + q$) and the equilibrium as described by R, q, and α. However, since $\tilde{\lambda} + \eta^2 \ll k^2$ the coefficient of J_1 is large while J_2 is at most of order unity. Therefore, $|J_1[(g_0)^{1/2}R)| \ll 1$, or to lowest order its argument must be

$$\sqrt{g_0}\, R = \sqrt{\frac{4q^2}{\tilde{\lambda} + \eta^2}\left(\frac{q^2\eta^2}{\tilde{\lambda} + \eta^2} - q_{cr}^2\right)}\, R \simeq j_{1,s} , \tag{33}$$

where $j_{1,s}$ is the sth zero of J_1. Solving for $\tilde{\lambda}$ gives dispersion relations for a spectrum of unstable eigenmodes indexed by s:

$$\tilde{\lambda} = -\eta^2 + \frac{2q^2R}{j_{1,s}}\left[-\frac{q_{cr}^2 R}{j_{1,s}} \pm \sqrt{\left(\frac{q_{cr}^2 R}{j_{1,s}}\right)^2 + \eta^2}\right] . \tag{34}$$

The eigenfunction (eq. [29]) corresponding to s has $s - 1$ zeros inside the tube.

The dispersion relationship above expresses growth rate, in the form of $\tilde{\lambda}$, as a function of wavenumber, expressed as η. The tube is unstable ($\tilde{\lambda} \geq 0$) over the narrow range of wavenumbers

$$|\eta| = |k + q| \leq \frac{\Delta k}{2} \equiv \frac{2qR}{j_{1,s}} \sqrt{q^2 - q_{cr}^2} , \tag{35}$$

centered on $k = -q$. Note that for the unstable perturbations, $|k + q| \ll q$ as initially assumed. The point of exact resonance, $\eta = 0$, is only marginally unstable ($\tilde{\lambda} = 0$) and the behavior is symmetric about this point. The maximum value is

$$\tilde{\lambda}_{\max,s} = \frac{R^2}{j_{1,s}^2}(q^2 - q_{cr}^2)^2 . \tag{36}$$

Returning to dimensional form, this corresponds to a maximum eigenfrequency of

$$\omega_{\max,s} = \pm i \frac{v_A R}{j_{1,s}}(q^2 - q_{cr}^2) . \tag{37}$$

This is smaller than the Alfvén frequency $v_A k$ by the factor $qR \ll 1$, justifying our earlier assumption. Of the spectrum of unstable modes, that corresponding to $s = 1$ ($j_{1,1} \simeq 3.83$) has the largest growth rate.

Figure 1 shows the weakly twisted eigenfunction $\xi_r(r)$, (eq. [29]) versus normalized radius r/R as the dotted curve. The solid curves show numerically computed eigenfunctions for strongly twisted tubes (§ 4). Even in the strongly twisted cases, the internal displacement is much larger than the displacement of the tube boundary. Thus the instability is primarily (though not entirely) internal. In the weakly twisted case, the radial boundary displacement $\xi_r(R)$ can be found by combining equations (29) and (32) to eliminate J_1,

$$\xi_r(R) = \frac{4R^2}{j_{1,s}^2}(q^2 - q_{cr}^2) J_2(j_{1,s}) . \tag{38}$$

Finally, we have

$$|\dot{\xi}_r(R)| = |2J_2(j_{1,s})/R| \gg |\xi_r(R)/R| \tag{39}$$

for this mode, in contrast to the stable Alfvén oscillation (transverse tube waves) which have essentially uniform displacement profiles.

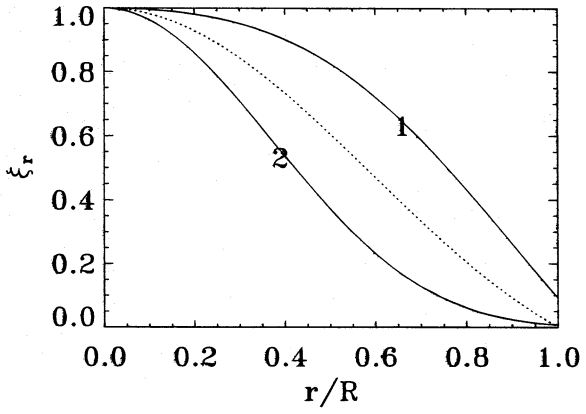

FIG. 1.—Unstable radial eigenmodes ξ_r. *Solid curve 1:* $qR = 1$, $B_z(r) = B_0$, $q_{cr}R = 0$. *Solid curve 2:* $qR = 1$, $B_z(r) = B_0(1 - r^2/R^2)^{0.36}$, $q_{cr}R = 0.6$. *Dotted curve:* $\xi_r(r) = 2J_1[(g_0)^{1/2}r]/(g_0)^{1/2}r$, from the weakly twisted limit: $qR \ll 1$, $B_z(r) = B_0(1 - \alpha r^2)$, $q_{cr}R = \alpha^{1/2}R$.

3.2. *Critical Twist (q_{cr}) for Strongly Twisted Tubes*

Analytical constraints can also be found for strongly twisted tubes. In the boundary condition (eq. [21]), the coefficients of $\xi_r(R)$ and $\dot{\xi}_r(R)$ are each positive when $\lambda > 0$ (instability). Thus to satisfy $D(\lambda; R, k) = 0$ it is necessary that $\xi_r(R)$ and $\dot{\xi}_r(R)$ be of opposite signs. Integrating the Euler-Lagrange equation (14) and noting that $f(0)\dot{\xi}(0) = 0$ gives

$$f(r)\dot{\xi}_r(r) = \int_0^r dr g(r)\xi_r(r) \, . \tag{40}$$

Since $f(r)$ (eq. [12]) is never negative when $\lambda > 0$, the expression above is inconsistent with $\xi_r(R)$ and $\dot{\xi}_r(R)$ of opposite sign unless $g(r)$ is negative somewhere. Thus a necessary condition for instability is that $g(r) < 0$ within $0 < r \leq R$.

For equilibria of the form (15) the necessary condition for instability $g(r) < 0$ can be cast as a lower bound on axial field gradient

$$\frac{dB_z}{dr} > \frac{rB_z}{2(1 + q^2r^2)}\left[\eta^2 - 4q^2 + \frac{2(k^2 - q^2)}{1 + k^2r^2}\right], \tag{41}$$

where we consider only marginal stability $\lambda = 0$. Tubes with axial gradients smaller (or more negative) than the right-hand side of equation (41) over the whole tube cross section are always stable. If $k = -q$, this is equivalent to Suydam's criterion (Suydam 1959), which indicates when a tube is unstable to a highly localized perturbation.

In cases of interest, the axial field is flat near the axis of the tube, and slopes more sharply at larger r. In this case, the gradient of B_z will be least negative near the axis, and equation (41) is most likely to be satisfied there. Expanding B_z as in equation (22) gives

$$\alpha < \tfrac{1}{4}\,[4q^2 - \eta^2 - 2(k^2 - q^2)] \text{ for instability} \, . \tag{42}$$

Close to resonance, $k + q = \eta \ll q$, the second and third terms in equation (42) are $\sim\eta^2$ and $\sim q\eta$, respectively, and can be dropped relative to $4q^2$. The condition for instability then reduces to the form of the criterion for instability in weakly twisted tubes, equation (30) ($q > q_{cr} \equiv \alpha^{1/2}$). In the strongly twisted case, however, this condition is merely sufficient since it is possible that equation (41) is satisfied away from the axis. In practice, this does not occur: § 4 shows agreement between the stability thresholds of weakly and strongly twisted tubes.

Numerical simulations shows this criterion to be inapplicable in the special case of a Gold-Hoyle field (Gold & Hoyle 1960). While the Gold-Hoyle field is at the margin of this condition ($q = \alpha^{1/2}$), we find it to be unstable for $-q < k < 0.17q$. In fact when $q^2 = \alpha$ it is necessary to retain higher powers of η in equation (42). Keeping these terms, equation (42) predicts instability for $-q < k < q/3$ in reasonable agreement with our numerical result. It also agrees with ranges of instability found in several other studies of Gold-Hoyle fields: $-q < k$ (Raadu 1972), $-q < k < q/3$ (Hood & Priest 1979), and $-q < k < 0.18q$ (Craig et al. 1990). Note also that because the instability of the Gold-Hoyle field is due to a higher order effect than instabilities for other tubes, its growth rate is correspondingly lower.

4. NUMERICAL RESULTS FOR STRONGLY TWISTED FLUX TUBES

For strongly twisted tubes we must solve equation (14) for $\xi_r(r)$ numerically. Given a $\boldsymbol{B}_0(r)$ profile and outer radius R, the method for finding an unstable eigenmode and its growth rate is as follows: Assume values for k and λ, and integrate equation (14) for ξ_r from $r = 0$ to the boundary at $r = R$. Generally, $D(\lambda; R, k) \neq 0$, and some form of iteration, e.g., the shooting method (see Press et al. 1986, p. 582), is used to vary λ for fixed k until $D(\lambda; R, k) = 0$. This results in the eigenfunction $\xi_\lambda(r)$ and eigenvalue λ, given $\boldsymbol{B}_0(r)$, k, and R. In general, there are multiple values of λ that satisfy the boundary conditions, forming a spectrum of eigenmodes, both stable (transverse tube waves) and unstable. Hereafter, we restrict ourselves to the most unstable mode, i.e., that with the largest value of λ for each $\boldsymbol{B}_0(r)$, k, and R.

The analytical results from § 3.1 were numerically confirmed in weakly twisted cases. A second class of profiles were then investigated to test the importance of an abrupt boundary at $r = R$. In these profiles $B_z(r)$ is flat in the center and goes continuously to zero. Growth rates and eigenfunctions $\xi_r(r)$ in these cases were close to those in the analytical (discontinuous) treatment.

Strongly twisted tubes of various profiles were then investigated. In all cases instability set in at a threshold equivalent to that found for weakly twisted tubes: $q_{cr} = \alpha^{1/2}$, where α is the coefficient of the r^2 term in a series expansion of B_z. One particular profile is

$$B_z = B_0\left(1 - \frac{r^2}{R^2}\right)^p, \tag{43}$$

where $p > 0$ so that B_z goes smoothly to zero at $r = R$. Taylor expansion $B_z = B_0(1 - pr^2/R^2 + \cdots)$ gives $q_{cr} = p^{1/2}/R$ which was verified by the numerical simulations, to within 0.5%. Near marginal stability this profile qualifies as weakly twisted only when $p \ll 1$. Another set of profiles uses a Bessel function $B_z = B(0)J_0(j_{0,1}r/R)$, which goes continuously to zero at $r = R$. Again, the threshold for instability was $q_{cr} = \alpha^{1/2} = j_{0,1}/(2R)$ to within 0.5%. We conclude that $q_{cr} = \alpha^{1/2}$ is a robust result for any tube where $B_\theta = qrB_z$, as is suggested by our analysis in § 3.2.

It has been argued (Parker 1979b, p. 172) that a tube is unstable when its magnetic tension drops to zero. For equation (43), zero tension occurs when $q = 2(p + 1)^{1/2}/R$, but the kink instability sets in at even smaller twist (i.e., $q = p^{1/2}/R$).

Further numerical investigations of strongly twisted flux tubes show qualitative, though not quantitative, agreement with the weakly twisted results. The solid curves in Figure 1 show two eigenmodes $\xi_r(r)$ for strongly twisted ($qR = 1$) tube profiles parameterized by p as in equation (43). Curve 1 is for a $p = 0$ profile, meaning B_z is perfectly flat out to $r = R$, and curve 2 is for a $p = 0.36$ profile. Both eigenmodes are the most unstable for their respective field profiles. (The less unstable modes look approximately like these modes, but are more concentrated toward the origin). The dotted curve in Figure 1 is the analytically derived eigenfunction given by equation (29) for a weakly twisted tube. The shape of ξ_r is qualitatively similar for all three cases, though the strongly twisted tubes have a greater amplitude near the outer boundary of the tube.

Figure 2 shows the eigenvalues for these same strongly twisted flux tubes. The points on these plots corresponding to the eigenfunctions of Figure 1 are indicated by the diamonds. The weakly twisted eigenvalues (eq. [34]) are shown by the dotted curves for these same tubes (although the

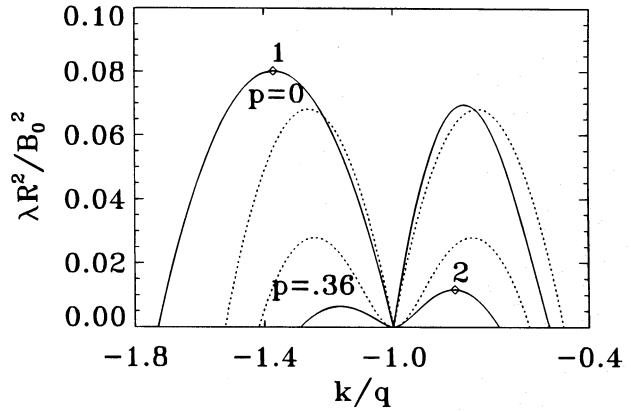

FIG. 2.—Dispersion relations for strongly twisted tubes $qR = 1$, with $B_z(r) = B_0(1 - r^2/R^2)^p$. *Solid curves:* numerically computed dispersion relations for tubes with $p = 0$ and $p = 0.36$. *Dotted curves:* analytical solution from the weakly twisted limit (eq. [34]) applied to the same two (strongly twisted) tubes. The values of k and λ for cases 1 and 2 shown in Fig. 1 are shown here by the diamonds labeled with the corresponding numbers.

assumptions leading to equation [34] are invalid here), showing that the qualitative behavior of strongly twisted tubes can be predicted from the analytical results of the weakly twisted case.

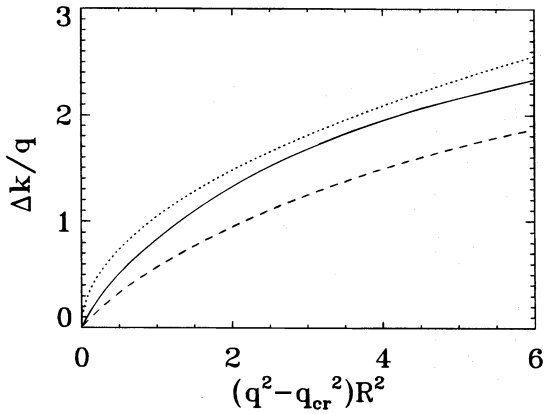

FIG. 3.—Δk = range of wavenumbers k over which tube is unstable. *Dotted curve:* $\Delta k/q = 4R(q^2 - q_{cr}^2)^{1/2}/3.83$, from the weakly twisted limit for $B_z = B_0(1 - q_{cr}^2 r^2)$. *Solid curve:* numerically computed range for $B_z = B_0(1 - r^2/R^2)^{0.36}$, $q_{cr}R = 0.6$. *Dashed curve:* numericaly computed range for $B_z = B_0(1 - r^2/R^2)$, $q_{cr}R = 1$.

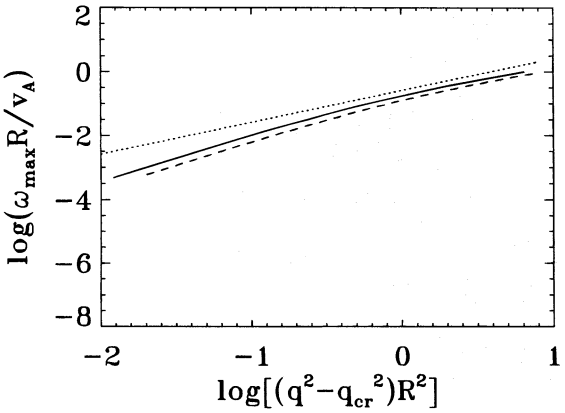

FIG. 4.—Behavior of growth rate as $(q^2 - q_{cr}^2)$ increases. *Dotted curve:* $\omega_{max}/v_A = R(q^2 - q_{cr}^2)/3.83$, from the weakly twisted limit for $B_z = B_0(0)(1 - q_{cr}^2 r^2)$. *Solid curve:* numerically computed growth rate for $B_z = B_0(0)(1 - r^2/R^2)^{0.36}$, $q_{cr} = 0.6$. *Dashed curve:* numerically computed growth rate for $B_z = B_0(0)(1 - r^2/R^2)$, $q_{cr}R = 1$.

Figures 3 and 4 show how the weakly twisted results can be used as a rough predictor for the range of unstable wavenumbers and the growth rates of strongly twisted flux tubes. The solid and dashed lines in Figure 3 show the relative range of k over which the strongly twisted tubes are unstable, $\Delta k/q$, versus $q^2 - q_{cr}^2$, for fields with $p = 0.36$ and $p = 1$, respectively. The dotted line shows the analytical prediction from equation (35). The solid and dashed lines in Figure 4 show ω_{max} versus $q^2 - q_{cr}^2$ for strongly twisted tubes, and the dotted line shows the results from equation (36). In both figures, the analytical weakly twisted results and numerical strongly twisted results agree in their general behavior, if not in their magnitude. For ω_{max}, we find that the weakly twisted prediction (eq. [37]) should be scaled down by a factor of $c_\omega \approx 2$–10 if it is applied to strongly twisted tubes.

5. THE DEVELOPMENT OF KINK-UNSTABLE FLUX LOOPS RISING THROUGH THE SOLAR CONVECTION ZONE

No one knows how twist is introduced into the toroidal fields that form new active regions. Observations of a large sample of active regions (Pevtsov, Canfield, & Metcalf 1995) made with the University of Hawaii's Haleakala Stokes Polarimeter (see Mickey 1985) show great variability in the helicity of individual active regions. Here, we simply assume that each toroidal magnetic flux tube is "born" with its own twist q. We presume that because a flux tube must be stable at the base of the convection zone, it is not initially twisted sufficiently to kink, i.e., $q < q_{cr}$. (We argue below that there is a minimum twist q_{min} which a flux tube must have to rise through the convection zone without fragmenting.)

Eventually a portion of the toroidal flux loop is destabilized, possibly by thermal transport of heat into the tube or by a gradual increase in the field strength as the fields are wound up by differential rotation. Once buoyantly unstable, the tube rises through the convection zone at a speed v_r which approximately balances buoyancy with aerodynamic drag (Parker 1979a)

$$v_r = v_A\left(\frac{\pi}{C_D}\right)^{1/2}\left(\frac{R}{\Lambda}\right)^{1/2}. \tag{44}$$

For a thin tube $R \ll \Lambda$ so $v_r \ll v_A$. How does the rising motion affect the distribution of twist along the tube? The azimuthal equation of motion for a section of a magnetic field line located at the coordinates (r, θ, z) in a tube with magnetic field (B_r, B_θ, B_z) gives

$$\rho r\frac{d^2\theta}{dt^2} = \frac{1}{4\pi}\left(B_z\frac{dB_\theta}{dz} + \frac{1}{r}B_\theta B_r + B_r\frac{dB_\theta}{dr}\right), \tag{45}$$

where all components of $\boldsymbol{B}$ are assumed independent of θ. Using $\nabla \cdot \boldsymbol{B} = 0$ and assuming $dB_z/dr = 0$ and $dB_r/dr \approx B_r/r$, we find

$$\frac{d^2\theta}{dt^2} = v_A^2\frac{d^2\theta}{dz^2}, \tag{46}$$

meaning that torsional forces propagate along the tube at the axial Alfvén speed

$$v_A \sim \sqrt{\frac{B_z^2}{4\pi\rho}}. \tag{47}$$

Because the rise speed is much less than the Alfvén speed, torsional forces will equilibrate quasi-statically, and the

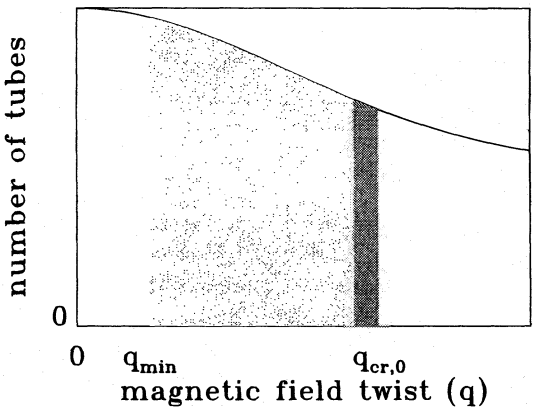

FIG. 5.—Sketch of hypothetical distribution of twists in flux tubes to illustrate effect of twist on tube evolution. For tubes with a given $B_z(r)$ and R, those with $q < q_{min}$ are destroyed by hydrodynamical forces as they rise, and those with $q > q_{cr,0}$ are destroyed by kinking before they begin to rise. Of tubes which can reach the photosphere (*all shaded areas*) those with q less than, but near $q_{cr,0}$ (*dark shaded area*) will kink.

right-hand side of equation (46) can be set to zero,

$$\frac{d}{dz}\frac{d\theta}{dz} = \frac{dq}{dz} = 0 . \tag{48}$$

Thus q is uniform as the tube rises, which also means that the axial current carried through the tube interior is conserved.

The quantity q should thus remain nearly constant and uniform along the tube during its rise. Meanwhile, because of gravitational stratification, the gas pressure confining the tube decreases substantially as the flux tube rises. The cross-sectional radius R must then increase in the rising portion of the tube. If the expansion occurs homologously in the directions normal to the tube axis, then the radial B_z profile will also expand homologously, resulting in a decrease of q_{cr} (i.e., $\propto^{1/2}$), with $q_{cr} \sim 1/R$.

The result is that the uppermost portion of the rising, twisted flux loop will become kink unstable when $q_{cr} \leq q$. As the tube continues to rise, an increasing fraction of the flux loop becomes kink unstable. This scenario is similar to the description of twisted flux loop evolution given by Parker (1979b, p. 186), but it differs in a crucial aspect: The kink is triggered *not* by an increase of twist at the apex of the flux loop, but rather by a flattening of the B_z profile (i.e., a decrease of q_{cr}) which occurs because of the expansion of the tube's cross section.

In addition to its role in the kink instability, magnetic twist may be important in preventing the dispersal or fragmentation of flux tubes during their rise through the solar convection zone. To maintain its integrity in the face of hydrodynamic forces the tube's circumferential tension force ($B_\theta^2/4\pi R$) must balance or exceed the hydrodynamic forces from flow past it ($\rho v_r^2/R$). This occurs when the rise speed is

$$v_r \lesssim v_{A,\perp} = \frac{B_\theta}{\sqrt{4\pi\rho}} = \frac{qRB_0}{\sqrt{4\pi\rho}} = qRv_A . \tag{49}$$

Combining equations (44) and (49) gives a minimum twist

$$q_{min} \gtrsim \frac{1}{\sqrt{R\Lambda}} \tag{50}$$

for the tube to maintain its integrity. The quantity q_{min} can be expressed in terms of q_{cr} as $q_{min} \simeq q_{cr}(R/\Lambda)^{1/2}$, where we assume the most kink stable case of $q_{cr} \simeq 1/R$. Because $(R/\Lambda)^{1/2} \ll 1$ near the base of the convection zone, there is a considerable range of twists for which the tube is both kink stable (before it emerges) and able to withstand the forces acting to break it apart.

The importance of the kink instability can be estimated by the number of e-foldings experienced by the tube as it rises one pressure scale height. With growth rate ω_{max} from equation (37), along with the factor c_ω (§ 4) to account for the difference between the strongly and weakly twisted growth rates, we find that the distance a tube will rise during the time it takes for a kink to go through one e-folding is

$$\frac{v_r}{|\omega_{max}|} \sim \frac{v_A\sqrt{R/\Lambda}}{v_A R(q^2 - q_{cr}^2)/c_\omega j_{1,1}} = c_\omega j_{1,1}\sqrt{R\Lambda}\,\frac{q_{min}^2}{q^2 - q_{cr}^2} . \tag{51}$$

This indicates that for a kink to go through one e-folding time while rising a distance shorter than a scale height, $q_{min}^2/(q^2 - q_{cr}^2)$ must be less than unity, or

$$q^2 \gtrsim q_{min}^2 + q_{cr}^2 . \tag{52}$$

As it is unlikely that tubes will have field profiles so flat that $q_{cr} \sim 0$, we expect that only tubes much more strongly twisted than the "minimally twisted" tube with $q = q_{min}$ will exhibit substantial kinking.

To illustrate these ideas we show a schematic picture of a hypothetical distribution of twists in flux tubes in Figure 5. Tubes with $q < q_{min}$ will be destroyed by hydrodynamical forces when they begin to rise from the base of the convection zone. Tubes with $q > q_{cr,0}$, where $q_{cr,0}$ is q_{cr} at the base of the convection zone, will be destroyed by kinking immediately after they are formed. Therefore tubes which can survive to rise to the photosphere and form active regions are those with $q_{min} < q < q_{cr,0}$, shown as the shaded regions in Figure 5. Of these tubes (which are all stable to kinking at the base of the convection zone) most will either remain king stable as they rise, or will not be kink unstable for long enough for the instability to significantly affect their geometry. However, those few tubes with q only slightly less than $q_{cr,0}$ will become kink unstable shortly after they begin rising and will have enough time to go through many instability e-folding times before they emerge. These tubes, represented by the dark shading in Figure 5, are therefore the ones which can emerge as knotted, flare-producing active regions.

6. CONCLUSIONS

A review of active region observations shows that some active regions appear to be formed by kinked or knotted flux tubes (Tanaka 1991; Kurokawa 1991; Kurokawa et al. 1994). These active regions are often the sources of the largest solar flares (Zirin 1988, p. 337) and are therefore of particular interest. One explanation for the structure of such flare-productive active regions is that they are flux tubes with highly twisted fields which become kink unstable below the photosphere. It is therefore important to understand the kink mode within the context of isolated, twisted flux tubes applied to the conditions of the solar interior. We investigated the simplest possible case of the isolated tube

so that we could understand the results as completely as possible.

We analyzed the kink instability using the energy principle, following many previous studies in tokomaks and in the solar corona, but with important differences: the boundary of the tube was coupled to the ideal flow of an external field-free plasma; the magnetic field was assumed to be pressure-confined; and the field pressure was assumed to be much less than the plasma pressure, i.e., $\beta \gg 1$, meaning that the fields are not generally force-free inside the tubes. Finally, we derived growth rates simultaneously with eigenfunctions for the unstable modes, whereas most past work has concentrated on deriving necessary or sufficient stability conditions (e.g., Suydam 1959; Hood & Priest 1980).

We found that the unstable eigenfunctions vary significantly over the cross section of the tube. In particular, the displacement for unstable perturbations was found to be largely internal, with motion at the outer edge of the tube much smaller than internal motion, though not zero. If the eigenfunction was forced to be constant across the tube, resulting in a helical translation of the entire tube, we found the tube to be stable. This means that an internal degree of freedom must be included in models of the evolution of twisted flux tubes to admit kinks.

For weakly twisted tubes ($qR \ll 1$), we derived growth rates and unstable eigenfunctions analytically. We found that unstable modes were those with axial wavelengths close to the axial magnetic field twist length. For both weakly and strongly twisted tubes, we solved numerically for unstable eigenfunctions and growth rates and found that the growth rates and range of unstable wave numbers for strongly twisted tubes can be predicted qualitatively by using analytical results from the weakly twisted case.

For all cases (weakly or strongly twisted) considered, we found it was necessary for the twist q to be greater than a critical twist q_{cr} for tubes to be kink unstable. The quantity q_{cr} was found to be $\alpha^{1/2}$, where α is the coefficient of the r^2 term in a Taylor series expansion of the axial magnetic field about the tube axis ($r = 0$): $B_z(r) = B_0(1 - \alpha r^2 + \cdots)$. Due to thermal, resistive, and viscous diffusion, it is likely that the magnetic field will decrease smoothly to zero from the axis to the edge of the tube, implying that $\alpha \sim 1/R^2$. Therefore only strongly twisted tubes ($qR \gtrsim 1$) will be kink unstable.

We show that as a tube rises, q will remain uniform, and $q_{cr} \sim 1/R$ will decrease, which allows tubes which are initially kink stable to become unstable as they rise. As tubes must be kink stable to remain in equilibrium at the base of the convection zone prior to emergence, we conclude that kink unstable (i.e., knotted, kinked) active regions form from rising flux loops which kink *after* emergence begins.

For strongly twisted tubes, the growth rates are large enough for the kink to go through one e-folding as it rises a distance small compared to the pressure scale height. This implies that the kink instability in strongly twisted tubes will develop to an extent that the tubes will be visibly deformed when they emerge into the photosphere, explaining the observations of Kurokawa et al. (1994), Tanaka (1991), Leka (1995), and others. However, our present work consists only of a linear analysis and is generally not be valid in the nonlinear regime. In particular, it is not clear whether the instability will remain internal, or if in its nonlinear development the internal motion will become large enough to extend beyond the tube boundary and essentially turn into an external kink. To determine the complete evolution of the instability, a fully nonlinear analysis needs to be done.

We wish to thank Sandy McClymont and K. D. Leka for useful discussions. M. G. L. was supported by NSF grant AST 92-18085 and NASA GSRP training grant NGT-51377. D. W. L. was supported by a fellowship from the Miller Institute for Basic Research in Science and by CalSpace grant CS-17-95. G. H. F. was supported by NASA grant NAGW-3429 and NSF grant AST 92-18085.

REFERENCES

Anzer, U. 1968, Sol. Phys., 3, 298
Bateman, G. 1978, MHD Instabilities (Cambridge: MIT Press)
Bernstein, I. B., Frieman, E. A., Kruskal, M. D., & Kulsrud, R. M. 1958, Proc. R. Soc. Lond. A, 244, 17
Caligari, P., Moreno-Insertis, F., & Schüssler, M. 1995, ApJ, 441, 886
Craig, I. J. D., Robb, T. D., Sneyd, A. D., & McClymont, A. N. 1990, Ap&SS, 166, 289
DeLuca, E., & Gilman, P. 1991, in Solar Interior and Atmosphere, ed. A. N. Cox, W. C. Livingston, & M. S. Matthews (Tucson: Univ. of Arizona Press), 275
D'Silva, S., & Choudhuri, A. 1993, A&A, 272, 621
Fan, Y., Fisher, G., & DeLuca, E. 1993, ApJ, 405, 390
Fan, Y., Fisher, G., & McClymont, A. 1994, ApJ, 436, 907
Ferriz-Mas, A., & Schüssler, M. 1990, in Physics of Magnetic Flux Ropes, ed. C. T. Russell, E. R. Priest, & L. C. Lee (Geophys. Monograph 58) (Washington: AGU), 141
Fisher, G. H., Fan, Y., & Howard, R. F. 1995, ApJ, 438, 463
Freidberg, J. P. 1987, Ideal Magnetohydrodynamics (New York: Plenum)
Gold, T., & Hoyle, F. 1960, MNRAS, 120, 89
Hood, A. W., & Priest, E. R. 1979, Sol. Phys., 64, 303
———. 1980, Sol. Phys., 66, 113
———. 1981, Geophys. Astrophys. Fluid Dyn., 17, 297
Hughes, D. W. 1992, in Sunspots, Theory and Observations, ed. J. H. Thomas & N. O. Weiss (Dordrecht: Kluwer), 371
Kruskal, M. D., Johnson, J. L., Gottlieb, M. D., & Goldman, L. M. 1958, Phys. Fluids, 1, 421
Kurokawa, H. 1991, Lecture Notes in Physics, 387, Flare Physics in Solar Activity Maximum 22, ed. Y. Uchida, R. C. Canfield, T. Watanabe, & E. Hiei (Berlin: Springer), 39
Kurokawa, H., Kitai, G., Shibata, K., Yafi, K., Ichimoto, K., Nitta, N., & Zhang, H. 1994, in Proc. Kofu Symposium (NRO Report No. 360), ed. S. Enome & T. Hirayama (Tucson: Univ. Arizona Press), 275
Leka, K. D. 1995, Ph.D. thesis, Univ. Hawaii
Longcope, D. W., Fisher, G. H., & Arendt, S. 1996, ApJ, 464, 999
Mickey, D. L. 1985, Sol. Phys., 97, 223
Migliuolo, S., & Cargill, P. J. 1983, ApJ, 271, 820
Moreno-Insertis, F. 1986, A&A, 166, 291
Moreno-Insertis, F., Caligari, P., & Schüssler, M. 1994, Sol. Phys., 153, 449
Newcomb, W. A. 1960, Ann. Phys., 10, 232
Parker, E. N. 1979a, ApJ, 230, 914
———. 1979b, Cosmical Magnetic Fields, Their Origin and Their Activity (Oxford: Clarendon Press)
Pevtsov, A. A., Canfield, R. C., & Metcalf, T. R. 1995, ApJ, 440, L109
Press, W. H., Flannery, B. P., Teukolsky, S. A., & Vetterling, W. T. 1986, Numerical Recipes: The Art of Scientific Computing (Cambridge: Cambridge Univ. Press)
Priest, E. R. 1984, Solar Magnetohydrodynamics (Boston: Reidel)
Raadu, M. A. 1972, Sol. Phys., 22, 425
Roberts, P. H. 1956, ApJ, 124, 430
Rosenbluth, M. N., Dagazian, R. Y., & Rutherford, P. 1973, Phys. Fluids, 16, 1894
Ryutov, D. A., & Ryutova, M. P. 1976, Sov. Phys.—JETP, 43, 491
Schüssler, M. 1979, A&A, 71, 79
Shafranov, V. D. 1957, J. Nucl. Energy II, 5, 86
Spruit, H. C. 1981, A&A, 98, 155
Suydam, B. R. 1959, in Proc. 2d U.N. Int. Conf. Peaceful Uses of Atomic Energy, 31 (Geneva: United Nations), 157
Tanaka, K. 1991, Sol. Phys., 136, 133
Voslamber, D., & Callebaut, D. K. 1962, Phys. Rev., 128, 2016
Zirin, H. 1988, Astrophysics of the Sun (Cambridge: Cambridge Univ. Press)